AGU PUBLICATIONS

Paleoceanography

RESEARCH ARTICLE
10.1002/2015PA002842

Key Points:
- Coherent salinity changes in the Agulhas Current and Indian-Atlantic Ocean Gateway (I-AOG)
- Salinity anomalies are not purely restricted to the Agulhas Current System itself
- Reduced salt flux via the I-AOG into the SE Atlantic during HS1

Supporting Information:
- Data Set S1
- Supporting Information S1

Correspondence to:
M. H. Simon,
margit.simon@uni.no

Citation:
Simon, M. H., X. Gong, I. R. Hall, M. Ziegler, S. Barker, G. Knorr, M. T. J. van der Meer, S. Kasper, and S. Schouten (2015), Salt exchange in the Indian-Atlantic Ocean Gateway since the Last Glacial Maximum: A compensating effect between Agulhas Current changes and salinity variations?, *Paleoceanography*, *30*, 1318–1327, doi:10.1002/2015PA002842.

Received 9 JUN 2015
Accepted 19 SEP 2015
Accepted article online 28 SEP 2015
Published online 28 OCT 2015

Salt exchange in the Indian-Atlantic Ocean Gateway since the Last Glacial Maximum: A compensating effect between Agulhas Current changes and salinity variations?

Margit H. Simon[1,2], Xun Gong[1,3], Ian R. Hall[1], Martin Ziegler[1,4], Stephen Barker[1], Gregor Knorr[1,3], Marcel T. J. van der Meer[5], Sebastian Kasper[5], and Stefan Schouten[4,5]

[1]School of Earth and Ocean Sciences, Cardiff University, Cardiff, UK, [2]Now at Uni Research Climate and Bjerknes Centre for Climate Research, Bergen, Norway, [3]Alfred Wegener Institute, Bremerhaven, Germany, [4]Faculty of Geosciences, Utrecht University, Utrecht, Netherlands, [5]Department of Marine Organic Biogeochemistry, NIOZ Royal Netherlands Institute for Sea Research, Den Burg, Netherlands

Abstract The import of relatively salty water masses from the Indian Ocean to the Atlantic is considered to be important for the operational mode of the Atlantic Meridional Overturning Circulation (AMOC). However, the occurrence and the origin of changes in this import behavior on millennial and glacial/interglacial timescales remains equivocal. Here we reconstruct multiproxy paleosalinity changes in the Agulhas Current since the Last Glacial Maximum and compare the salinity pattern with records from the Indian-Atlantic Ocean Gateway (I-AOG) and model simulations using a fully coupled atmosphere-ocean general circulation model. The reconstructed paleosalinity pattern in the Agulhas Current displays coherent variability with changes recorded in the wider I-AOG region over the last glacial termination. We infer that salinities simultaneously increased in both areas consistent with a quasi interhemispheric salt-seesaw response, analogous to the thermal bipolar seesaw in response to a reduced cross-hemispheric heat and salt exchange during times of weakened AMOC. Interestingly, these hydrographic shifts can also be recognized in the wider Southern Hemisphere, which indicates that salinity anomalies are not purely restricted to the Agulhas Current System itself. More saline upstream Agulhas waters were propagated to the I-AOG during Heinrich Stadial 1 (HS1). However, the salt flux into the South Atlantic might have been reduced due to a decreased volume transport through the I-AOG during the AMOC slowdown associated with HS1. Hence, our combined data-model interpretation suggests that intervals with higher salinity in the Agulhas Current source region are not necessarily an indicator for an increased salt import via the I-AOG into the South Atlantic.

1. Introduction

An increasing number of studies have focused on salt transport through the Indian-Atlantic Ocean Gateway (I-AOG), via the Agulhas leakage, which is considered as one potential controlling factor impacting on the North Atlantic salt budget [*Lutjeharms*, 2006; *Beal et al.*, 2011]. Agulhas leakage can be regarded as a by-product of variability within the Agulhas Current. The warm and saline Agulhas rings contribute salt and heat to the South Atlantic thermocline waters at a rate of up to 2.5×10^6 kg s^{-1} (salt) and 0.045 PW (heat), assuming a yearly total of six eddies [*van Ballegooyen et al.*, 1994], causing a salinity anomaly of +0.2 in the South Atlantic thermocline [*Gordon*, 1985]. The principal carrier of Agulhas leakage, the Agulhas rings, decays rapidly in the Cape Basin [*Schmid et al.*, 2003; *van Sebille et al.*, 2010], thereby losing their anomalous surface thermal content quickly to the atmosphere [*van Aken et al.*, 2003]. What remains is the enhanced salt content, which persists for longer and contributes to the overall densification of the South Atlantic on advective timescales [*Weijer et al.*, 2002; *Knorr and Lohmann*, 2003; *Biastoch et al.*, 2008; *Biastoch and Böning*, 2013]. The advection of salt is communicated north within two to four decades [*Weijer et al.*, 2002; *van Sebille et al.*, 2011; *Rühs et al.*, 2013], suggesting an immediate response of the Atlantic Meridional Overturning Circulation (AMOC) to the salt flux of Agulhas leakage with importance for global climate variability.

Enhanced transport of relatively saline water masses to the South Atlantic at the I-AOG is thought to be a key process during glacial terminations of Quaternary climate change by aiding the AMOC to its interglacial mode [*Knorr and Lohmann*, 2003; *Peeters et al.*, 2004; *Caley et al.*, 2012]. It has been shown that the

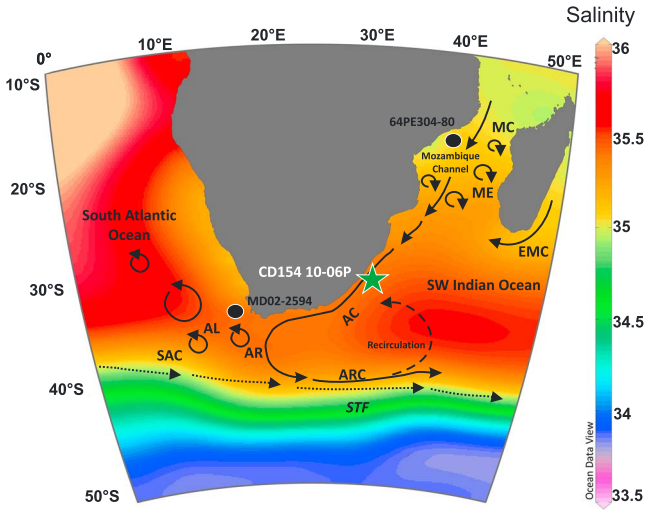

Figure 1. Location of the core CD154 10-06P this study (green star) and reference sites (black dots), I-AOG MD02-2594 [*Kasper et al*., 2014], 64PE304-80 [*Kasper et al*., 2015] in the Mozambique Channel, and oceanographic setting on a map of modern sea surface salinity. Mozambique eddies (ME), East Madagascar Current (EMC), Agulhas Current (AC), Agulhas Return Current (ARC), Agulhas Retroflection (AR), Agulhas Leakage in the form of Agulhas rings, and South Atlantic Current (SAC). The underlying map of modern sea surface salinity was compiled with high-resolution conductivity-temperature-depth data from http://www.nodc.noaa.gov and the Ocean Data View software version 4.3.7 by Schlitzer, R., Ocean Data View (http://odv.awi.de), 2010.

advection of excess salt from the subtropical South Atlantic and the tropics to the formation areas of North Atlantic Deep Water represent crucial contributions to shift the AMOC from a relatively weak (Heinrich-like) state to a stronger (Bølling-Allerød (B/A)-like) flow regime [*Knorr and Lohmann*, 2007; *Gong et al*., 2013]. Thus, it is crucial to understand what is driving the supply of salt to the South Atlantic over glacial terminations. Density changes in the southeast Atlantic can either be caused by an increasing amount of water being transferred through the I-AOG, i.e., more Agulhas leakage, or equally by more saline water derived from the Agulhas Current without changing leakage rates. Both scenarios would cause a change in the salinity signal recorded by paleoproxies from marine cores in the I-AOG without revealing the underlying mechanism. Therefore, the question arising is as follows: do proxy records in the I-AOG strictly represent Agulhas leakage (volume) variability or are the observed oscillations part of a wider South Atlantic-Southern Ocean signal during glacial terminations?

Here we explore this question by determining the nature of salinity changes in the wider Agulhas Current system. That is established by considering salinity variations within the two main components of the system: Agulhas Current and Agulhas leakage. We use marine sediment core CD154-10-06P (31°10.36'S, 032°08.91'E, 3076 m water depth, Figure 1) retrieved from the southwest Indian Ocean to study variations in salinity of the southern Agulhas Current since the Last Glacial Maximum (LGM; 19–23 kyr B.P.) [*Mix et al*., 2001]. These multiproxy paleosalinity records ($\delta D_{alkenone}$ and $\delta^{18}O_{seawater}$) are compared to reconstructions from the I-AOG previously interpreted to reflect changes in Agulhas salt leakage. Furthermore, model simulations [*Gong et al*., 2013] are reanalyzed to gain a larger-scale picture and to better understand what might have driven the observed salinity pattern in the Agulhas Current system.

2. Methods

2.1. Core Location and Regional Oceanography

The surface and thermocline waters above the core location are presently dominated by the Agulhas Current, which transports about 70–78 sverdrup (Sv) ($1\,Sv = 10^6\,m^3\,s^{-1}$) of tropical and subtropical waters along the southeastern coast of Africa from 27°S to 40°S [*Lutjeharms*, 2006]. These waters are characterized by high sea surface temperatures (23–26°C) and high surface salinities (35.4) [*Gordon et al*., 1987]. At the southern tip of Africa, between 15°E and 20°E, the current retroflects with the majority of its waters, about 70 to 75%, flowing back into the Indian Ocean as the Agulhas Return Current along the thermal subtropical front (Figure 1) [*Feron et al*., 1992]. Only the minority of this Agulhas Current's warm and salty waters, approximately 2–15 Sv, is transported into the South Atlantic through the I-AOG via Agulhas leakage [*de Ruijter et al*., 1999; *Richardson*, 2007]. As such the three components, Agulhas Current, Agulhas leakage, and Agulhas Return Current, are dynamically closely coupled and constitute the wider Agulhas Current system. The Agulhas Current system is fed by various water sources. Most of its water derives from the Mozambique Channel, from the southward flow to the east of Madagascar, from the Red Sea, and from inertial recirculation in the southwest Indian Ocean [*Beal et al*., 2006].

Studies have shown that the sources of the Agulhas Current are not dominated by the Mozambique Current [*Saetre and Da Silva*, 1984] or by the East Madagascar Current [*Lutjeharms*, 1988], but mostly by the recirculation in the southwest Indian Ocean subgyre (Figure 1) [*Stramma and Lutjeharms*, 1997].

2.2. Age Model CD154-10-06P

The age model for the core was developed using 10 ^{14}C accelerator mass spectrometer dates measured from samples containing approximately 1000 tests of *Globigerinoides ruber* (>250–315 μm). Radiocarbon measurements were made at the Natural Environment Research Council (NERC) Radiocarbon Laboratory (supporting information Table S1). The radiocarbon ages were converted into calendar years using the Marine09 data set [*Reimer et al*., 2009] with the global mean reservoir correction of (*R*) 405 years [*Bard*, 1988]. The core chronology was constructed using the statistical package BChron [*Parnell et al*., 2008, 2011] using a Bayesian approach to calculate the 95% (2σ) uncertainty on the calibrated ages (supporting information Table S1) and the 95% probability envelope for the time period studied (supporting information Figure S1). In the range of the ^{14}C dates (1.9–27.9 ka) relatively constant sedimentation rates of ~ 4.0 cm ka^{-1} (4.8–1.9 cm ka^{-1}) and a sample integration of ~300 years for every 1 cm sample is implied.

2.3. Inorganic Proxies

2.3.1. Planktonic Foraminifera δ^{18}O and Mg/Ca Measurements

Paired stable oxygen isotope (δ^{18}O) and Mg/Ca measurements in planktonic foraminifera species *G. ruber* are used to reconstruct changes in the surface salinities of the southern Agulhas Current (Figure 1). Around 30 individuals were picked from the 250–315 μm size fraction every 1 cm in the upper part of the core (0–76 cm).

Stable isotopes were measured using either a ThermoFinnigan MAT 252 mass spectrometer linked online to a Carbo Kiel-II carbonate preparation device (long-term external precision is 0.06‰ for δ^{18}O and 0.02‰ δ^{13}C) or a Thermo Scientific Delta V Advantage mass spectrometer coupled with a Gas Bench III automated preparation device (long-term external precision is 0.08‰ for δ^{18}O and 0.06‰ δ^{13}C) depending on the sample size. The stable isotope measurements were expressed relative to the Vienna Peedee Belemnite scale (VPDB) through calibration with the NBS-19 carbonate standard.

2.3.2. Mg/Ca Measurements

Magnesium-to-calcium ratio (Mg/Ca) measurements in planktonic foraminifer *G. ruber* have been used to reconstruct changes in the surface temperature of the Agulhas Current (Figure 1). *G. ruber* is a warm water species, highly abundant in the tropical-subtropical waters of the Indian Ocean and makes up to 40–60% of the planktonic foraminiferal assemblage of the Agulhas Current today [*Simon et al*., 2013]. A study of calcification depths of planktonic foraminifera in the tropical Indian Ocean showed that *G. ruber* calcifies within the mixed layer, between 20 and 50 m [*Mohtadi et al*., 2009]. Samples for Mg/Ca analysis were prepared and cleaned following the protocol outlined by *Barker et al*. [2003]. The samples were analyzed using a Thermo Element XR High inductively coupled plasma-mass spectrometry with a long-term precision of element ratios, determined by replicate analyses of standard solutions containing Mg/Ca = 1.15 mmol mol^{-1} and Mg/Ca = 6.9 mmol mol^{-1} of ±1.25% relative standard deviation (RSD) and ±0.52% RSD, respectively. The Mg/Ca ratios of *G. ruber* were converted to calcification temperature using the sediment trap calibration of *Anand et al*. [2003]: $T = (1/0.09) \times \ln((Mg/Ca)/0.449)$. The standard error associated with this calibration is ±1.1°C on the calcification temperature estimates (see supporting information for further details on trace elemental quality control and error propagation).

2.3.3. Seawater Oxygen Isotope Reconstruction ($\delta^{18}O_{sw}$)

The Mg/Ca-derived *G. ruber* calcification temperatures were used to determine the oxygen isotopic composition of seawater ($\delta^{18}O_{sw}$) by extracting the temperature component from the δ^{18}O of the calcite using the paleotemperature equation of *Kim and O'Neil* [1997], with a VPDB to Standard Mean Ocean Water δ^{18}O correction of 0.27‰ [*Hut*, 1987]. The $\delta^{18}O_{sw}$ was corrected for changes in global ice volume to produce ice-volume-corrected local $\delta^{18}O_{sw}$ estimates ($\delta^{18}O_{sw\text{-}ivc}$) following *Grant et al*. [2012] assuming a glacial δ^{18}O enrichment in seawater of 0.008‰ per meter sea level lowering [*Schrag et al*., 2002] (for details on uncertainties see supporting information).

2.4. Organic Proxies

2.4.1. δD of Alkenone Analysis

Similar to seawater δ^{18}O, seawater deuterium (D) content (δD) is also coupled to salinity with the δD being incorporated into algal biomarker lipids during photosynthesis reflecting the δD of sea water and salinity-dependent

biological fractionation amplifying the δD seawater effect [*Schouten et al*., 2006; *Chivall et al*., 2014; *M'boule et al*., 2014]. Thus, δD analyses on algal biomarker lipids could provide an alternative proxy for sea surface paleosalinity [*Schouten et al*., 2006]. Alkenone hydrogen isotope analyses were carried out on the ketone fraction using a Thermo-Finnigan DELTA V GC/TC/irMS Gas chromatograph (GC), thermal conversion (TC), isotope ratio monitoring (ir) mass spectrometer (MS) coupled with an Agilent GC using a GC Isolink and Conflo IV interface. Hydrogen isotope values for alkenones were standardized against pulses of H_2 reference gas, which was injected three times at the beginning and two times at the end of each run. Alkenone δD values were measured as the combined peak of the $C_{37:2}$ and $C_{37:3}$ alkenones [*van der Meer et al*., 2013], and the fractions were analyzed in duplicate if a sufficient amount of sample material was available. Standard deviations of replicate analyses varied from ±0.1‰ to ±5.9‰. A set of standard *n*-alkanes with known isotopic composition (Mix B prepared by A. Schimmelmann, University of Indiana) was analyzed daily prior to measuring samples in order to monitor system performance. Samples were only analyzed when the *n*-alkanes in Mix B had an average deviation from their offline determined value smaller than 5‰. The effect of changes in global ice volume on the $\delta D_{alkenone}$ were estimated by using the global mean ocean $\delta^{18}O_{sw}$ record from *Grant et al*. [2012] assuming a glacial $\delta^{18}O$ seawater of 0.008‰ per meter sea level lowering [*Schrag et al*., 2002]. The equivalent changes in $\delta^{18}O_{sw}$ were calculated by applying a local Indian Ocean meteoric waterline [*Srivastava et al*., 2010] which was subsequently subtracted from the $\delta D_{alkenone}$ record ($\delta D_{alkenone\text{-}ivc}$). Absolute salinity estimates are difficult to obtain from the $\delta D_{alkenone}$ due to the uncertainties in both the slope and intercept of the culture calibrations and other variables [*Rohling*, 2007]. Nevertheless, relative salinity changes from $\delta D_{alkenone}$ result can be roughly estimated since the slope of the $\delta D_{alkenone}$-salinity relationship is 4.8‰ for *E. huxleyi* and 4.2‰ for *G. oceanica* grown in batch cultures [*Schouten et al*., 2006].

2.5. Numerical Model Simulations

2.5.1. Atmosphere-Ocean General Circulation Model Simulations

In order to better evaluate the observed salinity changes during abrupt climate change in the wider Agulhas Current System, we reanalyze an Atmosphere-Ocean General Circulation Model (AOGCM) LGM experiment [*Zhang et al*., 2013; *Gong et al*., 2013], which applies a 0.2 Sv freshwater perturbation to the central North Atlantic Ocean 40°N–55°N, 45°W–20°W for 150 years. In this AOGCM experiment a state of suppressed AMOC (5 Sv) is reached by the end of the perturbation compared to the prehosing LGM equilibrium state (18 Sv). In section 3 the climate conditions associated with the suppressed AMOC state serve as a surrogate for the global climate conditions during Heinrich Stadial 1 (HS1).

3. Results and Discussion

3.1. Glacial-Interglacial Salinity Changes in the Agulhas Current and I-AOG Since the LGM

The ice-volume-corrected hydrogen isotopic composition of alkenones ($\delta D_{alkenone\text{-}ivc}$) in core CD 154 10-06P display an isotope shift from the LGM to the Holocene (core top) of approximately 10‰ with suborbital variability throughout the deglaciation (Figure 2b). Several factors can affect hydrogen isotope fractionation in haptophyte algae and the $\delta D_{alkenone}$ values including the following: (1) regional salinity change, (2) algal growth rate and growth phase, and (3) haptophyte species composition [*Schouten et al*., 2006; *Chivall et al*., 2014; *M'boule et al*., 2014]. The C_{37}/C_{38} alkenone ratio, indicative of haptophyte species composition [*Marlowe et al*., 1984; *Prahl et al*., 1988; *Schulz et al*., 2000], is very constant at 1.1 ± 0.1 throughout the record and does not seem to correlate with the $\delta D_{alkenone}$ (supporting information Figure S3). This suggests that $\delta D_{alkenone}$ is not affected by changes in species composition unlike a record form the Mozambique Channel where during the glacial the $\delta D_{alkenone}$ and C_{37}/C_{38} alkenone ratio covaried suggesting a species composition effect [*Kasper et al*., 2015].

Equal to the glacial-interglacial (G-I) changes evident in the $\delta D_{alkenone\text{-}ivc}$ data set an approximate 0.4‰ shift is displayed by the $\delta^{18}O_{sw\text{-}ivc}$ record (Figure 2c), derived from the same core material. Translating the observed LGM-Holocene changes to absolute salinities would suggest more saline waters in the southern Agulhas Current of approximately 1 during the LGM based on $\delta^{18}O_{sw\text{-}ivc}$ values. Based on the $\delta D_{alkenone\text{-}ivc}$ shift of approximately 10‰ the LGM would have been 2 more saline than the Holocene. Glacial-interglacial salinity changes in the Agulhas Current are generally accompanied by upper ocean temperature shifts of up to 4°C (Figure 2d). Comparison between the CD154 10-06P data set and *Kasper et al*. [2014] shows that the ice-volume-corrected residual $\delta D_{alkenone}$ recorded similar relative changes in salinity within the I-AOG and the Agulhas Current (CD154 10-06P site) with hydrogen isotope changes of approximately 10‰ since the LGM (Figure 2b). The general G-I trend from relatively elevated $\delta D_{alkenone\text{-}ivc}$ values during the LGM to lower

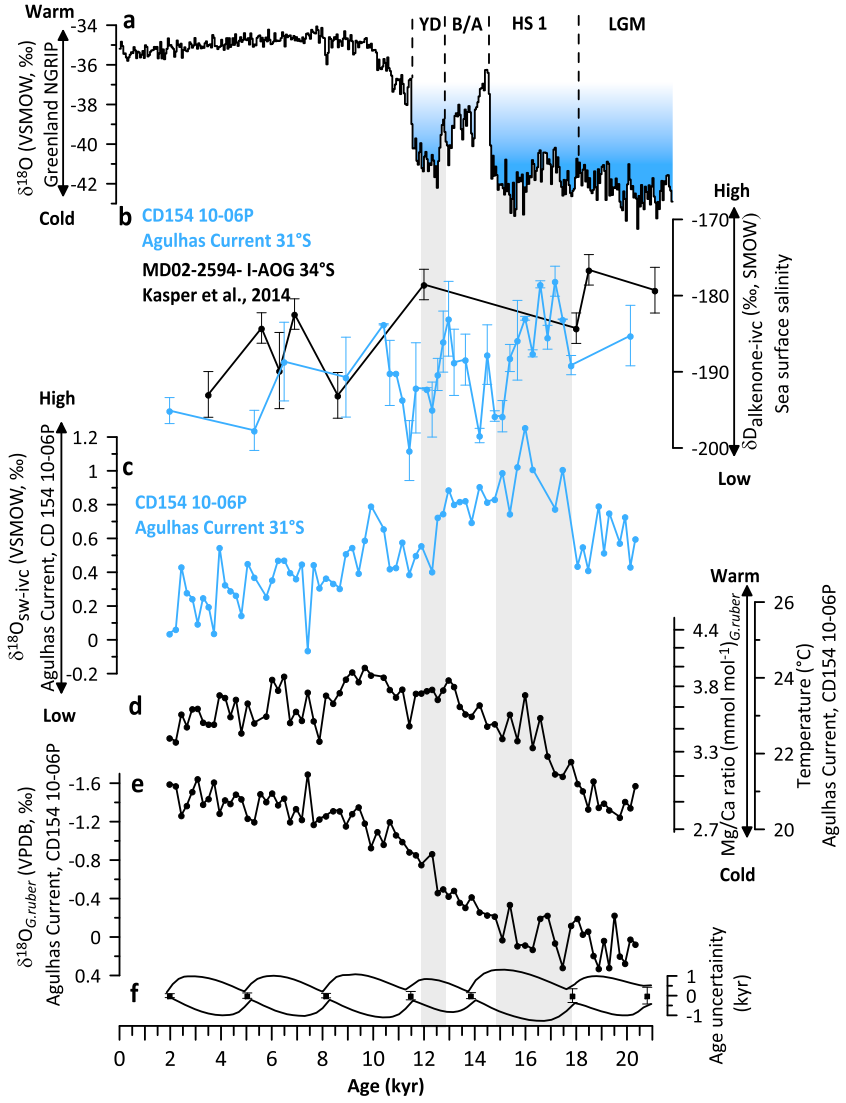

Figure 2. (a) $\delta^{18}O$ record from Greenland ice core *NGRIP* [2004], displaying abrupt temperature variability in the North Atlantic. Underlying grey bars indicate Last Glacial Maximum (LGM), Heinrich Stadial 1 (HS1), Bølling-Allerød interstadial (B/A), and Younger Dryas. (b) Hydrogen isotope composition of $C_{37:2-3}$ alkenones (blue,) for core CD154 10-06P reflecting sea surface salinity changes in the Agulhas Current and in the I-AOG core MD02-2594 (black) [*Kasper et al.*, 2014]. Error bars indicate 2 standard deviations based on replicate analyses of each sample. (c) Ice-volume-corrected $\delta^{18}O_{SW}$ reconstruction ($\delta^{18}O_{sw\text{-}ivc}$) for core CD154 10-06P. Propagated ($\pm 1\sigma$) error uncertainty associated to each data point is ±0.4‰. (d) Upper ocean temperature reconstruction at core location CD154 10-06P, derived from *G. ruber* Mg/Ca ratios using the equation of *Anand et al.* [2003]. (e) *Globigerinoides ruber* $\delta^{18}O$ profile for core CD154 10-06P. (f) Estimated uncertainties for the age model (calculated by Bchron [*Parnell et al.*, 2008]).

$\delta D_{alkenone\text{-}ivc}$ values during the Holocene is evident at both locations which implies that surface waters during the LGM within the I-AOG [*Kasper et al.*, 2014] as well as in the southern Agulhas Current were more saline than during the Holocene (Figure 2). Previous studies from the I-AOG observed elevated $\delta D_{alkenone\text{-}ivc}$ values [*Kasper et al.*, 2014], suggesting increased salinity, coinciding with assumed reduced Agulhas leakage (i.e., the volume transport of water from the Indian Ocean to the South Atlantic) during glacial stages [*Peeters et al.*, 2004]. If the amount of water exchanged between the two oceans was reduced during the LGM, one would expect the southwest Indian Ocean to become more saline in comparison to the South Atlantic due to increase residence time of Indian Ocean waters. However, the overall pattern in both $\delta D_{alkenone\text{-}ivc}$ records does not suggest that and might equally imply a downstream propagation of saltier (fresher) Agulhas Current waters during the LGM (Holocene) into the South Atlantic without any changes in leakage rates.

One could also consider that the G-I variability observed here in the southern Agulhas Current is a result of upstream source water changes, for example, in the Mozambique Channel (Figure 1). However, a recently published $\delta D_{alkenone}$ record from the core 64PE304-80 (18°14′26.6274″S; 37°52′8.6874″E, 1329 m water depth), located north of the Zambezi River Delta at the Mozambique shelf, shows no clear G-I shift in $\delta D_{alkenone}$ values [*Kasper et al.*, 2015]. It has been suggested that increased input of freshwater via the Zambezi River outflow [*Schefuß et al.*, 2011], either via closer proximity to the coast or increased precipitation or a combination of both, would lead to a lowering in δD_{sw} at the 64PE304-80 core site and subsequently to a decrease in $\delta D_{alkenone}$ during the glacial. The lack of a clear G-I salinity shift in the Agulhas Current source area (Mozambique Channel) [*Kasper et al.*, 2015] compared to the further downstream in the system (this study) moreover strengthens the assumption that upper ocean dynamics in the southern Agulhas Current area might have been crucial in determining the final leakage signature as opposed to its northern counterpart.

3.2. Millennial-Scale Salinity Changes in the Agulhas Current

The most recent transition from glacial to interglacial conditions (Termination I) encompassed several abrupt climatic shifts. Temperature records from Greenland and the North Atlantic are marked by a cold interval (Heinrich Stadial 1 (HS1)) during early Termination I (18–14.6 kyr ago)—a period associated with a massive ice-rafting episode known as Heinrich event 1. Thereafter an abrupt and significant warming occurred into the Bølling-Allerød (B/A). Rapidly following the B/A was the return to near-glacial conditions during the Younger Dryas (YD) event (12.8–11.5 kyr ago). Full interglacial conditions of the Holocene were reached by about 10 kyr ago.

During the course of the last deglaciation the $\delta D_{alkenone\text{-}ivc}$ values in core CD154 10-06P show a high degree of variability with the highest values during HS1, ranging from~−177 to −195‰, on average relatively higher than during the LGM. More specifically, in the first half of HS1 values ranging from ~−177 to −185‰ suggest relatively high salinity conditions at that time (Figure 2). In the second half of HS1 the $\delta D_{alkenone\text{-}ivc}$ values decreased to ~−195‰ at the end of and just after HS1, indicating a freshening of surface waters. During the B/A the $\delta D_{alkenone\text{-}ivc}$ values were initially relatively low suggesting lower salinity during this period compared to most of HS1 but increased toward the end of the B/A/YD transition to approximately −185‰. During the YD, the ice-volume-corrected alkenone δD values were initially high but decreased during the interval to approximately −195‰, suggesting relatively fresh conditions at the core site. After the YD, the hydrogen isotopic composition of the alkenones increase again, before slowly decreasing during the Holocene.

Variability in the $\delta^{18}O_{sw\text{-}ivc}$ record, derived from the same core material, is consistent with the pattern observed in the $\delta D_{alkenone\text{-}ivc}$ record (Figure 2c). The overall pattern in the $\delta^{18}O_{sw\text{-}ivc}$ data fits with the $\delta D_{alkenone\text{-}ivc}$ indicating higher salinities during the LGM compared to the Holocene. During Termination I, with the onset of HS1 the $\delta^{18}O_{sw\text{-}ivc}$ values display an abrupt shift toward higher values, indicative of enhanced salinities. With the end of HS1 and the onset of the B/A, isotope values decreased, suggesting freshening of the surface Agulhas Current; however, values remained higher compared to the YD interval. Thereafter, values continuously decreased toward the late Holocene values of ~0.4‰ in that record (Figure 2c). Salinity changes in the Agulhas Current were accompanied with rising upper ocean temperatures during HS1 and constant temperatures during the YD (Figure 2d).

Both proxies ($\delta D_{alkenone}$ and $\delta^{18}O_{sw}$) suggest that elevated salinity prevailed in the Agulhas Current during HS1 (Figure 2). Owing to the thermal bipolar seesaw behavior, the South Atlantic-Southern Ocean region warmed during Greenland stadials [*Broecker*, 1998; *Stocker and Johnsen*, 2003; *Barker and Diz*, 2014]. Elevated upper ocean temperatures during HS1 in the Agulhas Current are consistent with this pattern (Figure 2d). A warming in the South Atlantic-Southern Ocean region is accompanied by a salinification of the surface waters due to enhanced evaporation [*Lohmann*, 2003]. Analogous to the thermal bipolar seesaw [*Stocker and Johnsen*, 2003], *Lohmann* [2003], based on modeling results, suggested the presence of an additional quasi-bipolar salt-seesaw that reflects changes in the salt advection throughout the Southern Hemisphere supergyre in response to the interhemispheric seesaw. It is possible that the Agulhas Current hydrography was influenced by such a salt-seesaw mechanism causing the salinification of the upper water layers. The lower resolution of the I-AOG record [*Kasper et al.*, 2014] does not allow a direct comparison of both areas on shorter timescales over the last deglaciation. Notwithstanding, a previous comparison

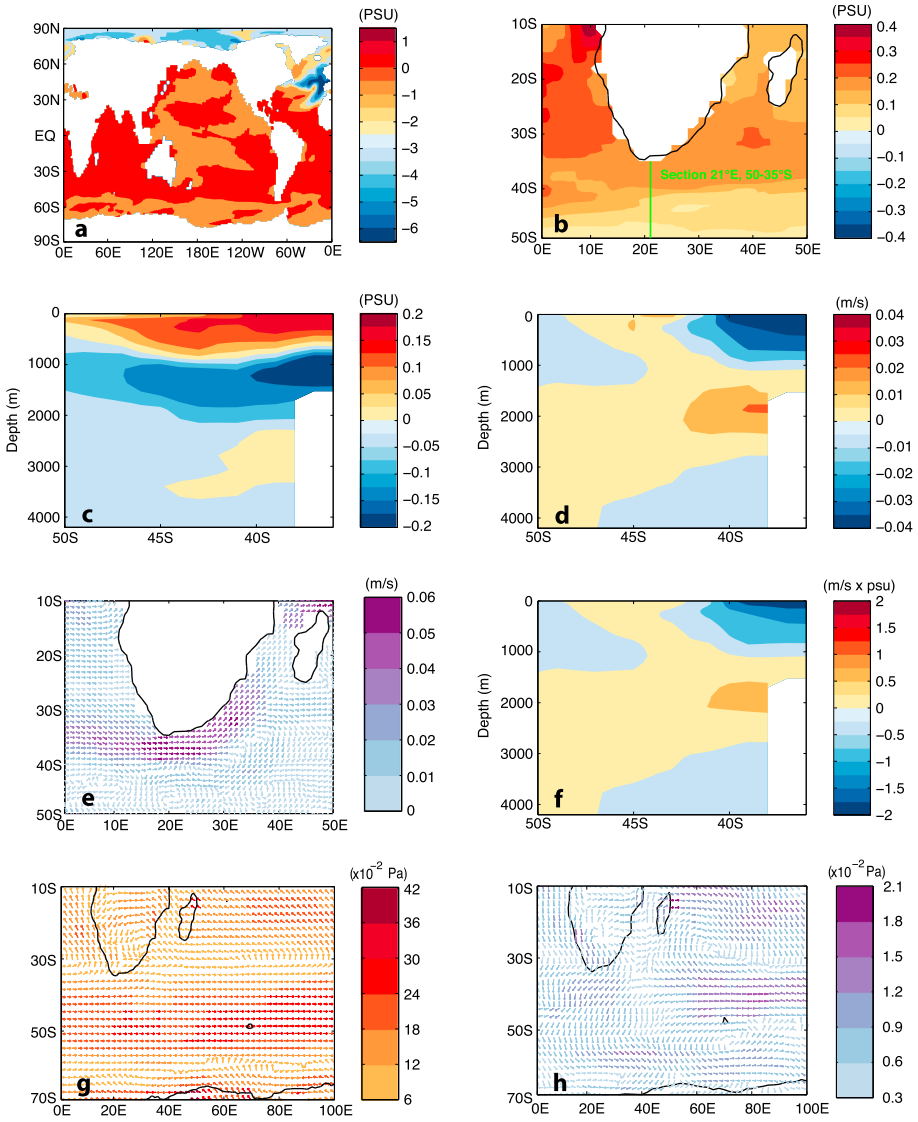

Figure 3. Modeling results of the LGM and HS1 experiments. The sea surface salinity anomalies of the HS1 to LGM state in (a) global ocean, (b) the region of the Agulhas Current and Indo-Atlantic Ocean gateway (I-AOG), (c) salinity, and (d) velocity anomalies within the water column at the 21°E, 50–35°S section of HS1 to LGM. Furthermore, the (e) surface velocity and (f) the salinity flux calculated by multiplying velocity and salinity in Figures 3c and 3d. (g) The LGM wind stress over the subtropical Southern Indian Ocean and (h) the wind stress anomaly between HS1 and LGM.

[*Simon et al.*, 2013] between the variability in the $\delta^{18}O_{sw}$ records in the Agulhas Current and the I-AOG [*Marino et al.*, 2013] during marine oxygen isotope stage 5 strengthened the assumption that the observed salinity oscillations in the I-AOG could be a result of propagated upstream changes in the Agulhas Current.

The transition from the B/A to the YD (~−13 ka) reveals the highest surface water salinities in the Agulhas Current during the latter half of Termination I (14.6–11.5 ka) with a pronounced freshening occurring throughout the rest of the YD (Figures 2b and 2c). Considering the uncertainties (±0.8 ka) associated with our age model across that interval (Figure 2f) the observed salinity peak in the B/A-YD transition could have occurred at the onset of the YD. In that case, it would suggest that there was, in fact, a similarity between salinity variations across HS1 and the YD, both intervals beginning with high sea surface salinity (SSS) followed by a decrease. However, absolute salinity values during HS1 were higher, which might be related to a more exaggerated climate perturbation during HS1, possibly in combination with decreasing background salinity throughout the deglaciation. Due to the complexities associated with deglaciation (e.g., changing

climate background state from glacial to interglacial, CO_2 levels) and uncertainty in the age model, we focus our ensuing discussion on the variability observed across HS1.

3.3. Simulated Changes in the Agulhas Realm and the Wider I-AOG Region

In order to test the general assumption that Northern Hemisphere climate variability forces hydrographical changes in the southwest Indian Ocean, an idealized North Atlantic freshwater perturbation experiment, analogous to the iceberg/meltwater discharge thought to be associated with a Heinrich Event [*Heinrich*, 1988], was reanalyzed (Figure 3) [*Gong et al*., 2013]. This numerical model simulation offers the opportunity to better evaluate the mechanism driving the observed salinity features in the multiproxy record of core CD154 10-06P. The I-AOG salinity flux around South Africa is controlled by two factors: ocean salinity changes and Agulhas Current velocities. In the following, we will discuss the individual change of each of these two factors, and ultimately their combined effect of the Indo-Atlantic salinity transport through the I-AOG.

Our model results show an increase in sea surface salinity (SSS) over the entire Southern Hemisphere Oceans including the Pacific; Indian and Atlantic Ocean sectors (Figure 3a). Around South Africa a uniform SSS increase of ~0.2 can be noticed in the region of the Agulhas Current and I-AOG (Figure 3b). Salinity increases in the upper water column down to intermediate depths in the I-AOG (Figure 3c). The average paleosalinity shift from the LGM to the HS1 mean state presented in this study (Figures 2b and 2c) is in general agreement with the modeled SSS changes from LGM to HS1 (Figure 3b). However, a direct comparison of absolute shifts between the data and model results should be taken with care due to (1) large uncertainties in the $\delta^{18}O_{sw}/\delta D_{alkenone}$-salinity relationship through time and (2) limitations of our idealized sensitivity experiment applied here.

The modeled global ocean salinity changes display that the salinity increase is not exclusively restricted to the Agulhas System but is rather a feature in the wider South Atlantic-Southern Ocean (Figure 3a). In fact, the signal is even more pronounced outside the Agulhas region, i.e., the equatorial South Atlantic and the northern Indian Ocean (Figures 3a and 3b). This appears in response to the reduction of the AMOC (forced in the experiments by North Atlantic freshwater). The slowdown of the AMOC results in a reduced transport of salt across the equator in the Atlantic Ocean, and a recirculation throughout the South Atlantic Subtropical gyre system [*Lohmann*, 2003]. This also results in a distribution of salt throughout the Southern Hemisphere supergyre and recirculation in the subtropical Indian Ocean Gyre system, effectively acting to increase salinity in the greater Agulhas region. Despite the fact that SSS is high (Figure 3c) the velocity section 21°E, 50–35°S reveals a slowdown in the water transport through the I-AOG at the same time, affecting the water column down to depth of ~1000 m (Figure 3d). Surface velocity anomalies of HS1 to LGM (Figure 3e) indicate reduced water volume transport of the Agulhas Current during the HS1. Compared to the increase of salinity, the reduction in speed of the Agulhas Current is a predominant factor and causes the reduction of westward salt flux through the I-AOG during the HS1 (Figure 3f).

To understand the underlying dynamics of the slowdown of the Agulhas Current during HS1, we show wind stress changes (Figures 3g and 3h) in the Indian Ocean associated with the North Atlantic freshwater perturbation. In the LGM state the modeled surface wind field (Figure 3g) is characterized by an anticlockwise (positive) wind stress curl over the subtropical Southern Indian Ocean driven by the southeasterly Trade Winds and Southern Hemisphere Westerlies. These latitudinal wind characteristics have been identified as the primary dynamic process of the Agulhas Current [*Beal et al*., 2011]. As shown in Figure 3h, the wind stress anomaly between HS1 and LGM characterizes a reduction in the positive wind stress curl over the subtropical Southern Indian Ocean, in agreement with a slowdown of the Agulhas Current during HS1. In the interval of a weak AMOC and weak Agulhas Current, the SSS shows a uniform increase in the region of the Agulhas Current and the wider I-AOG region. In our model simulation scenario this would result in a reduced salt flux to the South Atlantic via the I-AOG from the LGM to HS1 conditions. Dynamically, the slowdown of the Agulhas Current coincides with a reduction of the positive wind stress curl over the subtropical Southern Indian Ocean caused by the changes in southeasterly Trade Winds and Southern Hemisphere Westerlies in response to the AMOC slowdown.

4. Conclusions

The general agreement between the organically and inorganically derived proxy results confirms the application of $\delta D_{alkenone}$ for reconstructing past salinity changes in the wider Agulhas Current system. In detail,

we find evidence that oscillations in upper water mass salinities in the southern Agulhas Current since the LGM are important for finally determining the Agulhas salt leakage signal. That might imply that the Agulhas leakage signal south of Africa may, in fact, be controlled by upstream (southern Agulhas Current) dynamics, meaning that a change in the Agulhas leakage properties may occur even without a change in volume transport itself. In fact, more saline southern Agulhas Current waters were propagated to the I-AOG during times of abrupt climate change (HS1/weak AMOC states) explaining proxy evidence in both regions. However, due to a decreased volume transport through the I-AOG (according to our model results) at times of a weakened AMOC a reduced salt flux into the South Atlantic might have occurred. This implies that periods of higher salinity in the source region do not necessarily suggest that a greater fraction of Indian Ocean water entered the South Atlantic Ocean, as previously inferred from proxy records in the I-AOG.

Acknowledgments

We acknowledge funding from the European Commission 7th Framework Marie Curie People programme FP7/2007-2013 through funding of the Initial Training Network "GATEWAYS" (www.gateways itn.eu) under grant 238512 and the Climate Change Consortium of Wales. We thank Rainer Zahn, the captain, officers, and crew of RRS *Charles Darwin* cruise number 154, for which I.H. also gratefully acknowledge funding support from the Natural Environment Research Council. Marcel van der Meer was funded by the Dutch Organization for Scientific Research (NWO) through a VIDI grant, and Stefan Schouten was funded under the program of the Netherlands Earth System Science Centre (NESSC). Radiocarbon measurements were performed at the NERC Radiocarbon Facility, East Kilbride, UK. Furthermore, we acknowledge funding from the DAAD (German Academic Exchange Service) which supported the RISE (Research Internships in Science and Engineering) internship placement of Elisa Spreitzer who assisted together with Sebastian Steinig in carrying out laboratory and analytical work on core material CD154 10-06P. Alexandra Nederbragt, Lindsey Owen, and Anabel Morte-Ródenas provided technical support with the isotope and trace element analysis at Cardiff University. We thank Conor Purcell and Rainer Zahn for extensive discussions. We appreciate thoughtful comments provided by two anonymous reviewers. All data sets presented in this paper are tabulated within the supporting information.

References

Anand, P., H. Elderfield, and M. H. Conte (2003), Calibration of Mg/Ca thermometry in planktonic foraminifera from a sediment trap time series, *Paleoceanography*, *18*(2), 1050, doi:10.1029/2002PA000846.

Bard, E. (1988), Correction of accelerator mass spectrometry ^{14}C ages measured in planktonic foraminifera: Paleoceanographic implications, *Paleoceanography*, *3*(6), 635–645, doi:10.1029/PA003i006p00635..

Barker, S., and P. Diz (2014), Timing of the descent into the last Ice Age determined by the bipolar seesaw, *Paleoceanography*, *29*, 489–507, doi:10.1002/2014PA002623.

Barker, S., M. Greaves, and H. Elderfield (2003), A study of cleaning procedures used for foraminiferal Mg/Ca paleothermometry, *Geochem. Geophys. Geosyst.*, *4*(9), 8407, doi:10.1029/2003GC000559.

Beal, L. M., T. K. Chereskin, Y. D. Lenn, and S. Elipot (2006), The sources and mixing characteristics of the Agulhas Current, *J. Phys. Oceanogr.*, *36*(11), 2060–2074, doi:10.1175/JPO2964.1.

Beal, L. M., W. P. M. De Ruijter, A. Biastoch, and R. Zahn (2011), On the role of the Agulhas system in ocean circulation and climate, *Nature*, *472*(7344), 429–436, doi:10.1038/nature09983.

Biastoch, A., and C. W. Böning (2013), Anthropogenic impact on Agulhas leakage, *Geophys. Res. Lett.*, *40*, 1138–1143, doi:10.1002/grl.50243.

Biastoch, A., C. W. Boning, and J. R. E. Lutjeharms (2008), Agulhas leakage dynamics affects decadal variability in Atlantic overturning circulation, *Nature*, *456*(7221), 489–492, doi:10.1038/nature07426.

Broecker, W. S. (1998), Paleocean circulation during the last deglaciation: A bipolar seesaw?, *Paleoceanography*, *13*(2), 119–121, doi:10.1029/97PA03707.

Caley, T., J. Giraudeau, B. Malaizé, L. Rossignol, and C. Pierre (2012), Agulhas leakage as a key process in the modes of Quaternary climate changes, *Proc. Natl. Acad. Sci. U.S.A.*, *109*(18), 6835–6839, doi:10.1073/pnas.1115545109.

Chivall, D., D. M'Boule, D. Sinke-Schoen, J. S. Sinninghe Damsté, S. Schouten, and M. T. J. van der Meer (2014), The effects of growth phase and salinity on the hydrogen isotopic composition of alkenones produced by coastal haptophyte algae, *Geochim. Cosmochim. Acta*, *140*, 381–390, doi:10.1016/j.gca.2014.05.043.

de Ruijter, W. P. M., A. Biastoch, S. S. Drijfhout, J. R. E. Lutjeharms, R. P. Matano, T. Pichevin, P. J. V. Leeuwen, and W. Weijer (1999), Indian-Atlantic interocean exchange: Dynamics, estimation and impact, *J. Geophys. Res.*, *104*(C9), 20,885–20,910, doi:10.1029/1998JC900099.

Feron, R. C. V., W. P. M. De Ruijter, and D. Oskam (1992), Ring shedding in the Agulhas Current System, *J. Geophys. Res.*, *97*(C6), 9467–9477, doi:10.1029/92JC00736.

Gong, X., G. Knorr, G. Lohmann, and X. Zhang (2013), Dependence of abrupt Atlantic meridional ocean circulation changes on climate background states, *Geophys. Res. Lett.*, *40*, 3698–3704, doi:10.1002/grl.50701.

Gordon, A. L. (1985), Indian-Atlantic transfer of thermocline water at the Agulhas retroflection, *Science*, *227*(4690), 1030–1033, doi:10.1126/science.227.4690.1030.

Gordon, A. L., J. R. E. Lutjeharms, and M. L. Gründlingh (1987), Stratification and circulation at the Agulhas Retroflection, *Deep Sea Res., Part A*, *34*(4), 565–599, doi:10.1016/0198-0149(87)90006-9.

Grant, K. M., E. J. Rohling, M. Bar-Matthews, A. Ayalon, M. Medina-Elizalde, C. B. Ramsey, C. Satow, and A. P. Roberts (2012), Rapid coupling between ice volume and polar temperature over the past 150,000 years, *Nature*, *491*(7426), 744–747, doi:10.1038/nature11593.

Heinrich, H. (1988), Origin and consequences of cyclic ice rafting in the Northeast Atlantic Ocean during the past 130,000 years, *Quat. Res.*, *29*(2), 142–152, doi:10.1016/0033-5894(88)90057-9.

Hut, G. (1987), Consultants' group meeting on stable isotope reference samples for geochemical and hydrological investigations Rep. to Dir. Gen., Vienna, 16–18 September 1985, Int. At. Energy Agency, Vienna (1987), p. 42, 42.

Kasper, S., M. T. J. van der Meer, A. Mets, R. Zahn, J. S. Sinninghe Damsté, and S. Schouten (2014), Salinity changes in the Agulhas leakage area recorded by stable hydrogen isotopes of C_{37} alkenones during Termination I and II, *Clim. Past*, *10*(1), 251–260, doi:10.5194/cp-10-251-2014.

Kasper, S., M. T. J. van der Meer, I. S. Castañeda, R. Tjallingii, G.-J. A. Brummer, J. S. Sinninghe Damsté, and S. Schouten (2015), Testing the alkenone D/H ratio as a paleo indicator of sea surface salinity in a coastal ocean margin (Mozambique Channel), *Org. Geochem.*, *78*, 62–68, doi:10.1016/j.orggeochem.2014.10.011.

Kim, S.-T., and J. R. O'Neil (1997), Equilibrium and nonequilibrium oxygen isotope effects in synthetic carbonates, *Geochim. Cosmochim. Acta*, *61*(16), 3461–3475, doi:10.1016/S0016-7037(97)00169-5.

Knorr, G., and G. Lohmann (2003), Southern Ocean origin for the resumption of Atlantic thermohaline circulation during deglaciation, *Nature*, *424*(6948), 532–536.

Knorr, G., and G. Lohmann (2007), Rapid transitions in the Atlantic thermohaline circulation triggered by global warming and meltwater during the last deglaciation, *Geochem. Geophys. Geosyst.*, *8*, Q12006, doi:10.1029/2007GC001604.

Lohmann, G. (2003), Atmospheric and oceanic freshwater transport during weak Atlantic overturning circulation, *Tellus A*, *55*(5), 438–449, doi:10.1034/j.1600-0870.2003.00028.x.

Lutjeharms, J. R. E. (1988), Remote sensing corroboration of retroflection of the East Madagascar Current, *Deep Sea Res., Part A*, *35*(12), 2045–2050.

Lutjeharms, J. R. E. (2006), Three decades of research on the greater Agulhas Current, *Ocean Sci. Discuss.*, *3*(4), 939–995, doi:10.5194/osd-3-939-2006.

M'boule, D., D. Chivall, D. Sinke-Schoen, J. S. Sinninghe Damsté, S. Schouten, and M. T. J. van der Meer (2014), Salinity dependent hydrogen isotope fractionation in alkenones produced by coastal and open ocean haptophyte algae, *Geochim. Cosmochim. Acta*, *130*, 126–135, doi:10.1016/j.gca.2014.01.029.

Marino, G., R. Zahn, M. Ziegler, C. Purcell, G. Knorr, I. R. Hall, P. Ziveri, and H. Elderfield (2013), Agulhas salt-leakage oscillations during abrupt climate changes of the Late Pleistocene, *Paleoceanography*, *28*, 599–606, doi:10.1002/palo.20038.

Marlowe, I. T., J. C. Green, A. C. Neal, S. C. Brassell, G. Eglinton, and P. A. Course (1984), Long chain (n-C37–C39) alkenones in the Prymnesiophyceae. Distribution of alkenones and other lipids and their taxonomic significance, *Brit. Phycol. J.*, *19*(3), 203–216, doi:10.1080/00071618400650221.

Mix, A. C., E. Bard, and R. Schneider (2001), Environmental processes of the ice age: Land, oceans, glaciers (EPILOG), *Quat. Sci. Rev.*, *20*(4), 627–657, doi:10.1016/S0277-3791(00)00145-1.

Mohtadi, M., S. Steinke, J. Groeneveld, H. G. Fink, T. Rixen, D. Hebbeln, B. Donner, and B. Herunadi (2009), Low-latitude control on seasonal and interannual changes in planktonic foraminiferal flux and shell geochemistry off south Java: A sediment trap study, *Paleoceanography*, *24*, PA1201, doi:10.1029/2008PA001636.

NGRIP (2004), High-resolution record of Northern Hemisphere climate extending into the last interglacial period, *Nature*, *431*(7005), 147–151, doi:10.1038/nature02805.

Parnell, A. C., J. Haslett, J. R. M. Allen, C. E. Buck, and B. Huntley (2008), A flexible approach to assessing synchroneity of past events using Bayesian reconstructions of sedimentation history, *Quat. Sci. Rev.*, *27*(19–20), 1872–1885, doi:10.1016/j.quascirev.2008.07.009.

Parnell, A. C., C. E. Buck, and T. K. Doan (2011), A review of statistical chronology models for high-resolution, proxy-based Holocene palaeoenvironmental reconstruction, *Quat. Sci. Rev.*, *30*(21–22), 2948–2960, doi:10.1016/j.quascirev.2011.07.024.

Peeters, F. J. C., R. Acheson, G.-J. A. Brummer, W. P. M. de Ruijter, R. R. Schneider, G. M. Ganssen, E. Ufkes, and D. Kroon (2004), Vigorous exchange between the Indian and Atlantic Oceans at the end of the past five glacial periods, *Nature*, *430*(7000), 661–665, doi:10.1038/nature02785.

Prahl, F. G., L. A. Muehlhausen, and D. L. Zahnle (1988), Further evaluation of long-chain alkenones as indicators of paleoceanographic conditions, *Geochim. Cosmochim. Acta*, *52*(9), 2303–2310, doi:10.1016/0016-7037(88)90132-9.

Reimer, P. J., et al. (2009), IntCal09 and Marine09 radiocarbon age calibration curves, 0–50,000 years cal BP, *Radiocarbon*, *51*, 1111–1150.

Richardson, P. L. (2007), Agulhas leakage into the Atlantic estimated with subsurface floats and surface drifters, *Deep Sea Res., Part I*, *54*(8), 1361–1389, doi:10.1016/j.dsr.2007.04.010.

Rohling, E. J. (2007), Progress in paleosalinity: Overview and presentation of a new approach, *Paleoceanography*, *22*, PA3215, doi:10.1029/2007PA001437.

Rühs, S., J. V. Durgadoo, E. Behrens, and A. Biastoch (2013), Advective timescales and pathways of Agulhas leakage, *Geophys. Res. Lett.*, *40*, 3997–4000, doi:10.1002/grl.50782.

Saetre, R., and A. J. Da Silva (1984), The circulation of the Mozambique channel, *Deep Sea Res., Part A*, *31*(5), 485–508.

Schefuß, E., H. Kuhlmann, G. Mollenhauer, M. Prange, and J. Patzold (2011), Forcing of wet phases in southeast Africa over the past 17,000 years, *Nature*, *480*(7378), 509–512, doi:10.1038/nature10685.

Schmid, C., O. Boebel, W. Zenk, J. R. E. Lutjeharms, S. L. Garzoli, P. L. Richardson, and C. Barron (2003), Early evolution of an Agulhas ring, *Deep Sea Res., Part II*, *50*(1), 141–166, doi:10.1016/S0967-0645(02)00382-X.

Schouten, S., J. Ossebaar, K. Schreiber, M. V. M. Kienhuis, G. Langer, A. Benthien, and J. Bijma (2006), The effect of temperature, salinity and growth rate on the stable hydrogen isotopic composition of long chain alkenones produced by *Emiliania huxleyi* and *Gephyrocapsa oceanica*, *Biogeosciences*, *3*(1), 113–119, doi:10.5194/bg-3-113-2006.

Schrag, D. P., J. F. Adkins, K. McIntyre, J. L. Alexander, D. A. Hodell, C. D. Charles, and J. F. McManus (2002), The oxygen isotopic composition of seawater during the Last Glacial Maximum, *Quat. Sci. Rev.*, *21*(1–3), 331–342, doi:10.1016/s0277-3791(01)00110-x.

Schulz, H.-M., A. Schöner, and K.-C. Emeis (2000), Long-chain alkenone patterns in the Baltic Sea—An ocean-freshwater transition, *Geochim. Cosmochim. Acta*, *64*(3), 469–477, doi:10.1016/S0016-7037(99)00332-4.

Simon, M. H., K. L. Arthur, I. R. Hall, F. J. C. Peeters, B. R. Loveday, S. Barker, M. Ziegler, and R. Zahn (2013), Millennial-scale Agulhas Current variability and its implications for salt-leakage through the Indian–Atlantic Ocean Gateway, *Earth Planet. Sci. Lett.*, *383*, 101–112, doi:10.1016/j.epsl.2013.09.035.

Srivastava, R., R. Ramesh, R. A. Jani, N. Anilkumar, and M. Sudhakar (2010), Stable oxygen, hydrogen isotope ratios and salinity variations of the surface Southern Indian Ocean waters, *Curr. Sci.*, *99*(10), 1395–1399.

Stocker, T. F., and S. J. Johnsen (2003), A minimum thermodynamic model for the bipolar seesaw, *Paleoceanography*, *18*(4), 1087, doi:10.1029/2003PA000920.

Stramma, L., and J. R. E. Lutjeharms (1997), The flow field of the subtropical gyre of the South Indian Ocean, *J. Geophys. Res.*, *102*(C3), 5513–5530, doi:10.1029/96JC03455.

van Aken, H. M., A. K. van Veldhoven, C. Veth, W. P. M. de Ruijter, P. J. van Leeuwen, S. S. Drijfhout, C. P. Whittle, and M. Rouault (2003), Observations of a young Agulhas ring, Astrid, during MARE in March 2000, *Deep Sea Res., Part II*, *50*(1), 167–195, doi:10.1016/s0967-0645(02)00383-1.

van Ballegooyen, R., M. L. Gründlingh, and J. R. E. Lutjeharms (1994), Eddy fluxes of heat and salt from the southwest Indian Ocean into the southeast Atlantic Ocean: A case study, *J. Geophys. Res.*, *99*, 14,053–14,070.

van der Meer, M. T. J., A. Benthien, J. Bijma, S. Schouten, and J. S. Sinninghe Damsté (2013), Alkenone distribution impacts the hydrogen isotopic composition of the $C_{37:2}$ and $C_{37:3}$ alkan-2-ones in *Emiliania huxleyi*, *Geochim. Cosmochim. Acta*, *111*, 162–166, doi:10.1016/j.gca.2012.10.041.

van Sebille, E., P. J. van Leeuwen, A. Biastoch, and W. P. M. de Ruijter (2010), On the fast decay of Agulhas rings, *J. Geophys. Res.*, *115*, C03010, doi:10.1029/2009JC005585.

van Sebille, E., L. M. Beal, and W. E. Johns (2011), Advective time scales of Agulhas leakage to the North Atlantic in surface drifter observations and the 3D OFES model, *J. Phys. Oceanogr.*, *41*(5), 1026–1034, doi:10.1175/2011JPO4602.1.

Weijer, W., W. P. M. De Ruijter, A. Sterl, and S. S. Drijfhout (2002), Response of the Atlantic overturning circulation to South Atlantic sources of buoyancy, *Global Planet. Change*, *34*(3–4), 293–311, doi:10.1016/S0921-8181(02)00121-2.

Zhang, X., G. Lohmann, G. Knorr, and X. Xu (2013), Different ocean states and transient characteristics in Last Glacial Maximum simulations and implications for deglaciation, *Clim. Past*, *9*(5), 2319–2333, doi:10.5194/cp-9-2319-2013.